# Compatibility of Boundary Angular Velocities in the Velocity-based 3D Beam Formulation

Eva Zupan and Dejan Zupan
Faculty of Civil and Geodetic Engineering
University of Ljubljana
Ljubljana, Slovenia
Email: eva.zupan.lj@gmail.com; dejan.zupan@fgg.uni-lj.si

***Abstract*—In this paper, a new velocity-based finite element approach for non-linear dynamics of beam-like structures is introduced. In contrast to standard approaches we here base the formulation on velocities and angular velocities expressed in the most suitable basis regarding standard approximation and interpolation techniques. The additivity of angular velocities in local frame description brings several benefits, such as trivial discretization and update procedure for the primary unknowns and improved stability properties of the time integrator. On the other hand, different initial orientations of elements connected together lead to nodal angular velocities that are expressed in different frames and cannot be directly equalized. The compatibility of angular velocities over the finite element boundaries thus needs to be solved. We avoid introducing constraint equations and additional degrees of freedom and introduce a computationally cheap solution instead.**

***Keywords–non-linear dynamics; spatial beams; finite-element method; boundary conditions; velocity-based approach; continuity of velocities.***

## I. INTRODUCTION

The total set of equations in solid mechanics consists of non-linear equilibrium, kinematic and constitutive equations that need to be solved for displacements, strains and stresses. Many practical problems in solid mechanics deal with structures that have one dimension larger than the other two, e.g., columns and girders in civil engineering, robotic arms, rotor blades and aircraft wings in mechanical engineering, deoxyribonucleic acid (DNA) molecules in biology and medicine, nanotubes in nanotechnology. Such structures are usually modelled as beams. It is of utmost importance to consider properly the boundary and continuity conditions when proposing a novel finite element (FE) beam model [1]. We focus in this paper on a structure of a velocity based beam element and the computational aspects in satisfying the continuity conditions over the boundaries.

The paper is structured as follows. Section II presents the oveview of the beam formultions, while Section III introduces the governing equations of the Cosserat beam model. In Section IV, we describe a novel numerical solution method for Cosserat beams. The treatment of boundary conditions is presented in Section V. In Section VI, some numerical examples are given. The paper ends with concluding remarks.

## II. BEAM FORMULATIONS

For beam-like structures the kinematics of a body becomes simplified but the equations remain non-linear, see, e.g., Antman [2], Reissner [3] and Simo [4]. Additionally, the reduced kinematics introduces the three-dimensional rotations of rigid cross-sections to describe the configuration of a beam. Spatial rotations are often taken to be the primary variables in three-dimensional beam formulations, see, e.g., [4]–[15], despite their demanding mathematical structure. In the solution algorithms for beams many authors reduce the total set of equations in such a way that the configuration variables (displacements and rotations) become the only unknowns of the problem. For numerical solution methods, such reduction means that the configuration variables need to be discretized with respect to space and time. The multiplicative nature of rotations, characterized by non-additivity, orthogonality and non-commutativity, needs to be properly considered in the numerical solution methods to gain a sufficient performance of calculations and accuracy of the results. Such demands highly increase the complexity of algorithms and disable direct applicability of the methods developed for standard Euclidean spaces, see, e.g., [16]–[21].

Mathematically, rotations are linear transformations in three-dimensional Euclidean space and can therefore be represented by $3 \times 3$ matrices. However, these nine components have six constraints, which makes a matrix representation of rotations less convenient for numerical implementations. Widely used are the three-parameter representations of which the often chosen "rotational vector" [22] is only one among many possibilities. It is well known that all three-parameter descriptions of rotations posses singularities. To avoid them a four parameter representations were also used, e.g., [23]–[25]. Surprisingly, it was only recently that this ideas were successfully revived, see, e.g., [14], [15], [26]–[29]. In this paper, rotational quaternions will be used as a suitable representation of rotations, but they will not be taken to be the primary unknowns of the problem. From the perspective of total mechanical energy of the system the velocities and angular velocities seem to be more natural quantities.

Thus, the alternative approach employed here exploits computationally simpler angular velocities as the primary quantities for the description of rotational degrees of freedom. Such approach brings several advantages to non-linear beam dynamics:

- when expressed in local bases, the components of angular velocity vector become additive, which enables the use of standard discretization and interpolation techniques;
- the stability of implicit time integrators is improved by taking the derivative of configuration quantities as the iterative unknowns, see Hosea and Shampine [30];
- the time discretization, linearization of equations and the update procedure are much simpler compared to standard beam elements.

Besides its advantages, this new approach brings some novel issues that need to be properly solved. The crucial idea of the finite element method (FEM) lies in subdivision of a larger structure into smaller parts called finite elements. An important part of the solution procedure is the assembly of equations of finite elements into a larger system of equations that describe the problem at the structural level. The simplest assumption used in the assembly procedure is that the elements are rigidly connected so that the displacements and rotations are continuous over the boundaries. When the displacements and rotations are chosen as the primary variables, a simple Boolean identification of degrees of freedom can be used. This yields that velocities and angular velocities are continuous over the finite element boundaries as well, but only when expressed with respect to a fixed basis.

For the sake of computational advantages at the element level, we express the angular velocities with respect to the moving frame. Because of this choice, the simple identification of degrees of freedom that belongs to the joints between elements can no longer be used due to different initial orientations of elements. Thus, the continuity of configuration quantities in a fixed frame leads to a more complicated relation in the local frame. This relation could be introduced at the structural level using the method of Lagrange multipliers, but such an approach would increase the number of degrees of freedom and the computational complexity of the overall algorithm. An elegant and computationally cheap alternative is presented here. Excellent properties of the proposed numerical model are demonstrated by numerical examples.

## III. COSSERAT BEAM MODEL

Among beam models, the *Cosserat theory of rods*, [2], is widely used. The numerical implementation of the model is usually attributed to Reissner [3] and Simo [4], where it is also called *the geometrically exact beam*. Only a brief description of the model is presented here.

The centroidal line $\left\{\vec{r}\,(x,t)\,,\ x\in[0,L]\,,\ t\geq 0\right\}$ and the family of cross-sections $\{\mathcal{A}\,(x,t)\,,\ x\in[0,L]\,,\ t\geq 0\}$ of the beam are parametrized by the arc-length parameter $x$ and the time $t$, where $L$ is the length of the beam in its initial position, see Figure 1. We assume that cross-sections are bounded plane regions that preserve their shape and area during deformation.

For the description of beam equations and the quantities therein, we introduce the *local* orthonormal basis

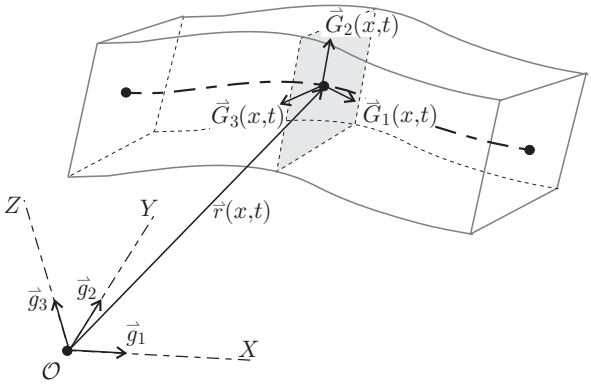


Figure 1. A three-dimensional beam.

$\left\{\vec{G}_1\,(x,t)\,,\vec{G}_2\,(x,t)\,,\vec{G}_3\,(x,t)\right\}$, which defines the orientation of each cross-section, and the *global* orthonormal basis $\left\{\vec{g}_1,\vec{g}_2,\vec{g}_3\right\}$, which is fixed in time and space. A rotation between the global and the local basis, defined by the quaternion multiplication $(\circ)$ reads

$$\vec{G}_i\,(x,t)=\widehat{q}\,(x,t)\circ\vec{g}_i\circ\widehat{q}^{\,*}\,(x,t)\,,\qquad i=1,2,3, \tag{1}$$

where $\widehat{q}$ denotes the rotational quaternion and $\widehat{q}^{\,*}$ its conjugate. A comprehensive presentation of the quaternion algebra can be found, e.g., in the textbook [31]. For more details on the application of quaternions in beam models please refer to [32] or [15].

Note that any rotational quaternion $q$ has a firm physical meaning. It be presented as the sum of a scalar and a vector,

$$\widehat{q}=\cos\frac{\vartheta}{2}+\sin\frac{\vartheta}{2}\,\vec{n}\,,\qquad \left|\vec{n}\right|=1, \tag{2}$$

where $\vartheta$ denotes the angle of rotation and $\vec{n}$ is the unit vector on the axis of rotation.

In what follows abstract vectors will be replaced by component representations. The bold-face letters will be used to represent vector quantities in the component form. The lower case letters will be used when a vector is expressed with respect to the fixed frame and the upper case letters are used for the local basis description. A hat over the letter denotes a four-dimensional vector, a member of the algebra of quaternions. The dependency of quantities on space $x$ and time $t$ will be mostly omitted for better readability.

### A. Kinematic compatibility

In Cosserat rod theory the resultant strain measures at the centroid of each cross-section are directly introduced and expressed with kinematic variables by the first order differential equations

$$\boldsymbol{\Gamma}=\widehat{\mathbf{q}}^{\,*}\circ\mathbf{r}'\circ\widehat{\mathbf{q}}+\boldsymbol{\Gamma}_0, \tag{3}$$

$$\mathbf{K}=2\widehat{\mathbf{q}}^{\,*}\circ\widehat{\mathbf{q}}', \tag{4}$$

where $\mathbf{\Gamma}$ and $\mathbf{K}$ denote the translational and rotational strain, respectively, both expressed with respect to the local basis. The prime $(')$ denotes the derivative with respect to $x$. Similarly, when we measure the rate of change of configuration variables with time, we have

$$\mathbf{v} = \dot{\mathbf{r}}, \tag{5}$$

$$\mathbf{\Omega} = 2\widehat{\mathbf{q}}^{*} \circ \dot{\widehat{\mathbf{q}}}, \tag{6}$$

introducing velocity $\mathbf{v}$ in fixed basis and angular velocity $\mathbf{\Omega}$ in local basis description, while the dot denotes the time derivative. It is important to observe that strains, velocities, and angular velocities are mutually dependent. Their direct relation is obtained by comparing mixed partial derivatives. After a straightforward derivation, we have

$$\dot{\mathbf{\Gamma}} = \widehat{\mathbf{q}}^{*} \circ \mathbf{v}' \circ \widehat{\mathbf{q}} + (\widehat{\mathbf{q}}^{*} \circ \mathbf{r}' \circ \widehat{\mathbf{q}}) \times \mathbf{\Omega}, \tag{7}$$

$$\dot{\mathbf{K}} = \mathbf{\Omega}' + \mathbf{K} \times \mathbf{\Omega}. \tag{8}$$

Equations (7)–(8) describe the kinematic compatibility of continuous system, [33], [34]. Its importance is obvious: the relation between the rotational strains and the angular velocities is described without rotational parameters. Since the rotational degrees of freedom are usually highly non-linear when compared to other quantities such modification of kinematic equations can be numerically advantageous.

### *B. Governing equations*

The continuous balance equations of a three-dimensional beam in quaternion notation read:

$$\mathbf{n}' + \tilde{\mathbf{n}} = \rho A \dot{\mathbf{v}}, \tag{9}$$

$$\mathbf{m}' + \mathbf{r}' \times \mathbf{n} + \tilde{\mathbf{m}} = \mathbf{q} \circ \left( \mathbf{J}_\rho \dot{\mathbf{\Omega}} + \mathbf{\Omega} \times \mathbf{J}_\rho \mathbf{\Omega} \right) \circ \widehat{\mathbf{q}}^{\,*}. \tag{10}$$

Equation (9) is a standard linear momentum balance equation, while equation (10) represents the angular momentum balance equation in terms of quaternion algebra as it follows from the generalized d'Alembert principle considering the unit norm of rotational quaternion. Here, $\mathbf{n}$ and $\mathbf{m}$ are the resultant force and moment vector of the cross-section expressed in fixed frame, i.e.,

$$\mathbf{n}\,(x,t) = \widehat{\mathbf{q}}\,(x,t) \circ \mathbf{N}\,(x,t) \circ \widehat{\mathbf{q}}^{\,*}\,(x,t)\,, \tag{11}$$

$$\mathbf{m}\,(x,t) = \widehat{\mathbf{q}}\,(x,t) \circ \mathbf{M}\,(x,t) \circ \widehat{\mathbf{q}}^{\,*}\,(x,t)\,, \tag{12}$$

where $\mathbf{N}$ and $\mathbf{M}$ are the same vectors expressed in local basis; $\rho$ is the density of the material; $A$ is the area of the cross-section; $\mathbf{J}_\rho$ is the matrix of mass moments of inertia; $\tilde{\mathbf{n}}$ and $\tilde{\mathbf{m}}$ are vectors of applied distributed force and moment. Together with balance equations the following conditions at the boundaries need to be satisfied:

$$\mathbf{n}(0,t) + \mathbf{f}^0\,(t) = \mathbf{0}, \tag{13}$$

$$\mathbf{m}(0,t) + \mathbf{h}^0\,(t) = \mathbf{0}, \tag{14}$$

$$\mathbf{n}(L,t) - \mathbf{f}^L\,(t) = \mathbf{0}, \tag{15}$$

$$\mathbf{m}(L,t) - \mathbf{h}^L\,(t) = \mathbf{0}, \tag{16}$$

$\mathbf{f}^0$, $\mathbf{h}^0$, $\mathbf{f}^L$ and $\mathbf{h}^L$ are the external time-dependent point forces and moments at the two boundaries, $x = 0$ and $x = L$.

For constitutive equations various models could be taken, but here we limit ourselves to the simplest case of linear elastic material, where

$$\mathbf{N} = \mathrm{diag}\,[\ EA \quad GA_2 \quad GA_3\ ]\,\mathbf{\Gamma}, \tag{17}$$

$$\mathbf{M} = \mathrm{diag}\,[\ GI_1 \quad EI_2 \quad EI_3\ ]\,\mathbf{K}. \tag{18}$$

Here, $EA/L$ is the axial stiffness, $EI_2$ and $EI_3$ denote the bending stiffness, $GI_1/L$ is the torsional stiffness, $GA_2$ and $GA_3$ are the shear stiffnesses.

## IV. NUMERICAL SOLUTION METHOD

We will solve the balance equations using the method of weighted residuals. Equations (9) and (10) are multiplied by test functions $I_p\,(x)$, $p = 1, 2, ..., N$, and integrated along the length of the beam:

$$\int_0^L \left[ \mathbf{n}' - \tilde{\mathbf{n}} - \rho A \ddot{\mathbf{r}} \right] I_p \, dx = \mathbf{0}, \tag{19}$$

$$\int_0^L \Big[ \mathbf{m} - (\mathbf{r}' \times \mathbf{n}) - \tilde{\mathbf{m}} - \widehat{\mathbf{q}} \circ \left( \mathbf{J}_\rho \dot{\mathbf{\Omega}} \right) \circ \widehat{\mathbf{q}}^{\,*} I_p + \mathbf{\Omega} \times (\widehat{\mathbf{q}} \circ (\mathbf{J}_\rho \mathbf{\Omega}) \circ \widehat{\mathbf{q}}^{\,*}) \Big] I_p \, dx = \mathbf{0}. \tag{20}$$

The terms $\mathbf{n} I_p$ and $\mathbf{m} I_p$ are integrated by parts, which after considering the boundary conditions (13)–(16) gives:

$$\int_0^L \left[ \mathbf{n} I_p' - \tilde{\mathbf{n}} I_p + \rho A \ddot{\mathbf{r}} I_p \right] dx - \delta_p \boldsymbol{f} = \mathbf{0}, \tag{21}$$

$$\int_0^L \Big[ \mathbf{m} I_p' - (\mathbf{r}' \times \mathbf{n})\, I_p - \tilde{\mathbf{m}} I_p + \widehat{\mathbf{q}} \circ \left( \mathbf{J}_\rho \dot{\mathbf{\Omega}} \right) \circ \widehat{\mathbf{q}}^{\,*} I_p + \boldsymbol{\omega} \times (\widehat{\mathbf{q}} \circ (\mathbf{J}_\rho \mathbf{\Omega}) \circ \widehat{\mathbf{q}}^{\,*})\, I_p \Big] dx - \delta_p \boldsymbol{h} = \mathbf{0}. \tag{22}$$

Here

$$\delta_p \mathbf{f} = \begin{cases} \mathbf{f}^0, & p = 1 \\ \mathbf{f}^L, & p = N \\ 0, & \text{otherwise} \end{cases}, \qquad \delta_p \mathbf{h} = \begin{cases} \mathbf{h}^0, & p = 1 \\ \mathbf{h}^L, & p = N \\ 0, & \text{otherwise} \end{cases}.$$

Equations (21)–(22) represent a system of $6N$ algebraic equations that is in general too demanding to be solved analytically. In our approach, we express all the unknown quantities with velocity and angular velocity. The approximative solution in both time and space is then spanned on these two quantities. for completeness the details on discretization will be briefly introduced.

### A. Time discretization

For the time discretization, we use the approximation of displacements at $t_{n+1}$ following from the mean value theorem:

$$\mathbf{r}^{[n+1]} = \mathbf{r}^{[n]} + h\frac{\mathbf{v}^{[n]} + \mathbf{v}^{[n+1]}}{2},$$

which yields

$$\mathbf{r}^{[n+1]} = \mathbf{r}^{[n]} + h\overline{\mathbf{v}},$$

where $\overline{\mathbf{v}}$ denotes the average velocity

$$\overline{\mathbf{v}} = \frac{\mathbf{v}^{[n]} + \mathbf{v}^{[n+1]}}{2}$$

and $h = t_{n+1} - t_n$ is the time step of the scheme.

For accelerations we can similarly employ

$$\frac{\mathbf{a}^{[n]} + \mathbf{a}^{[n+1]}}{2} = \frac{\mathbf{v}^{[n+1]} - \mathbf{v}^{[n]}}{h}.$$

After some rearrangement of terms, the scheme for translational degrees of freedom reads

$$\begin{aligned}
\mathbf{r}^{[n+1]} &= \mathbf{r}^{[n]} + h\overline{\mathbf{v}},\\
\mathbf{v}^{[n+1]} &= -\mathbf{v}^{[n]} + 2\overline{\mathbf{v}},\\
\mathbf{a}^{[n+1]} &= -\mathbf{a}^{[n]} - \frac{4}{h}\mathbf{v}^{[n]} + \frac{4}{h}\overline{\mathbf{v}}.
\end{aligned} \tag{23}$$

This scheme can be interpreted as a modification of the classical implicit Newmark scheme, where the average velocity becomes the iterative unknown, see [8] and [35].

A similar approach can be used for rotational degrees of freedom with an important exception stemming from the nonlinear relationship between angular velocities and rotational quaternions. The exponential mapping is used to map from incremental angular velocities to incremental rotations. The incremental rotation is then multiplied with the current one. The scheme for rotational degrees of freedom reads

$$\begin{aligned}
\widehat{\mathbf{q}}^{[n+1]} &= \widehat{\mathbf{q}}^{[n]} \circ \exp\left(\frac{h}{2}\overline{\mathbf{\Omega}}\right),\\
\mathbf{\Omega}^{[n+1]} &= -\mathbf{\Omega}^{[n]} + 2\overline{\mathbf{\Omega}},\\
\boldsymbol{\alpha}^{[n+1]} &= -\boldsymbol{\alpha}^{[n]} - \frac{4}{h}\mathbf{\Omega}^{[n]} + \frac{4}{h}\overline{\mathbf{\Omega}},
\end{aligned} \tag{24}$$

where exp denotes the quaternion exponential

$$\exp(\widehat{\mathbf{x}}) = \widehat{\mathbf{1}} + \frac{\widehat{\mathbf{x}}}{1!} + \frac{1}{2!}\widehat{\mathbf{x}} \circ \widehat{\mathbf{x}} + \frac{1}{3!}\widehat{\mathbf{x}} \circ \widehat{\mathbf{x}} \circ \widehat{\mathbf{x}} + .... \tag{25}$$

The above presented time-discretization scheme describes the assumptions taken regarding displacements, rotations and their time derivatives. For deformable structures time discretization of strain quantities is also needed. We derive the discrete compatibility equations analogously as for the continuous case. This gives

$$\begin{aligned}
\mathbf{\Gamma}^{[n+1]} = \exp^*\left(\frac{h}{2}\overline{\mathbf{\Omega}}\right) \circ \left(\mathbf{\Gamma}^{[n]} - \mathbf{\Gamma}_0\right) \exp\left(\frac{h}{2}\overline{\mathbf{\Omega}}\right)\\
+ h\widehat{\mathbf{q}}^{*[n+1]} \circ \overline{\mathbf{v}}' \circ \widehat{\mathbf{q}}^{[n+1]} + \mathbf{\Gamma}_0,
\end{aligned} \tag{26}$$

$$\begin{aligned}
\mathbf{K}^{[n+1]} = \exp^*\left(\frac{h}{2}\overline{\mathbf{\Omega}}\right) \circ \mathbf{K}^{[n]} \circ \exp\left(\frac{h}{2}\overline{\mathbf{\Omega}}\right)\\
+ 2\exp^*\left(\frac{h}{2}\overline{\mathbf{\Omega}}\right) \circ \exp'\left(\frac{h}{2}\overline{\mathbf{\Omega}}\right).
\end{aligned} \tag{27}$$

When the governing equations of a beam are evaluated at discrete time $t_{n+1}$ and the schemes (23)–(24) are taken into account, we obtain the system of equations dependent only on the arch-length parameter $x$. In order to solve these equations at each particular time step we need to introduce the spatial discretization.

### B. Spatial discretization

After the time discretization introduced, the average velocities $\overline{\mathbf{v}}$ and $\overline{\mathbf{\Omega}}$ are the only unknown functions along the length of the beam for any particular discrete time. They are replaced by a set of nodal values $\overline{\mathbf{v}}^p$, $\overline{\mathbf{\Omega}}^p$ at discretization points $x_p$, $p = 1, \ldots, N$, with $x_1 = 0$ and $x_N = L$, and interpolated by a set of interpolation functions $I_p(x)$ in-between:

$$\overline{\mathbf{v}}(x) = \sum_{p=1}^{N} I_p(x)\,\overline{\mathbf{v}}^p, \tag{28}$$

$$\overline{\mathbf{\Omega}}(x) = \sum_{p=1}^{N} I_p(x)\,\overline{\mathbf{\Omega}}^p. \tag{29}$$

The same discretization procedure is performed at every finite element of the structure. Thus, boundary nodes $x_1$ and $x_N$ become members of the global notes important at the structural level, while $x_2$,... $x_{N-1}$ are internal points of the element, often but not necessarily condensed at the elements level. Angular velocities in local basis description are additive quantities and the standard aditive-type interpolation used is in complete accord with the properties of the configuration space.

### C. Newton iteration

After time and space discretization, the governing equations (21)–(22) are replaced by a set of nonlinear algebraic equations that need to be solved at each discrete time for all the nodal values. The non-linear equations are solved iteratively using the Newton-Raphson method

$$\mathbf{K}^{[i]}\delta\mathbf{y} = -\mathbf{f}^{[i]}, \tag{30}$$

where $\mathbf{K}^{[i]}$ is the global Jacobian tangent matrix, $\mathbf{f}^{[i]}$ the residual vector of discretized equations (21)–(22), both in iteration $i$, and $\delta\mathbf{y}$ a vector of corrections of all nodal unknowns

$$\delta\mathbf{y} = \begin{bmatrix} \delta\overline{\mathbf{v}}_1 & \delta\overline{\mathbf{\Omega}}_1 & \cdots & \delta\overline{\mathbf{v}}_M & \delta\overline{\mathbf{\Omega}}_M \end{bmatrix}^T$$

A suitable choice of nodal variables allows the kinematically admissible additive update:

$$\overline{\mathbf{v}}^{[i+1]} = \overline{\mathbf{v}}^{[i]} + \delta\overline{\mathbf{v}}, \tag{31}$$

$$\overline{\boldsymbol{\Omega}}^{[i+1]} = \overline{\boldsymbol{\Omega}}^{[i]} + \delta\overline{\boldsymbol{\Omega}} \tag{32}$$

at each discrete point of the structure. Further details on linearization of equations can be found in [36].

## V. Continuity of boundary values

Finite elements have equal displacements and rotations at the rigid joints. However, the initial rotations of different elements are not necessarily equal. When the initial orientations differ, we need to distinguish between the initial and the relative rotations. Let us start with two elements having different initial orientations, described by quaternions $\widehat{\mathbf{q}}_0^{\mathrm{I}}$ and $\widehat{\mathbf{q}}_0^{\mathrm{II}}$ at the joint: $\widehat{\mathbf{q}}_0^{\mathrm{I}} \neq \widehat{\mathbf{q}}_0^{\mathrm{II}}$. When the joint is rigid the position vectors are equal, but the total rotations differ

$$\mathbf{r}^{\mathrm{I}} = \mathbf{r}^{\mathrm{II}} \qquad \text{and} \qquad \widehat{\mathbf{q}}^{\mathrm{I}} \neq \widehat{\mathbf{q}}^{\mathrm{II}}, \tag{33}$$

as shown in Figure 2.

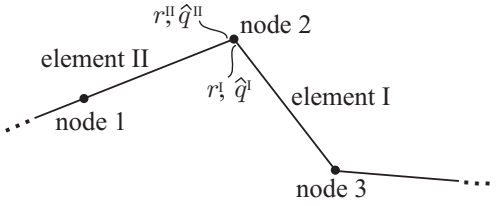


Figure 2. A rigid joint of two differently oriented elements.

The total rotations can be expressed as a composition of initial and relative rotation

$$\widehat{\mathbf{q}}^{\mathrm{I}} = \widehat{\mathbf{q}}_0^{\mathrm{I}} \circ \widehat{\mathbf{k}}^{\mathrm{I}} \qquad \text{and} \qquad \widehat{\mathbf{q}}^{\mathrm{II}} = \widehat{\mathbf{q}}_0^{\mathrm{II}} \circ \widehat{\mathbf{k}}^{\mathrm{II}}, \tag{34}$$

where the relative rotations are equal:

$$\widehat{\mathbf{k}}^{\mathrm{I}} = \widehat{\mathbf{k}}^{\mathrm{II}}. \tag{35}$$

The continuity condition, which could also be called the compatibility of rotations at the element boundaries, thus reads

$$\widehat{\mathbf{q}}^{\mathrm{I}} \circ \widehat{\mathbf{q}}_0^{\mathrm{I}*} = \widehat{\mathbf{q}}^{\mathrm{II}} \circ \widehat{\mathbf{q}}_0^{\mathrm{II}*}.$$

In configuration based approach we usually avoid enforcing this condition by introducing the relative rotational quaternion $\widehat{\mathbf{k}}$ as the nodal variable. For the velocity-based approach, we can similarly observe that

$$\overline{\mathbf{v}}^{\mathrm{I}} = \overline{\mathbf{v}}^{\mathrm{II}} \qquad \text{and} \qquad \overline{\boldsymbol{\Omega}}^{\mathrm{I}} \neq \overline{\boldsymbol{\Omega}}^{\mathrm{II}},$$

as the angular velocities are expressed in different local frames. We will derive the compatibility condition for angular velocities at the joints and propose a similar strategy as for rotational quaternions to avoid the use of Lagrange multipliers method by the substitution of the primary unknowns of Newton's iteration at the structural level. The details are presented in the sequel.

### A. Relation between boundary angular velocities

The angular velocity vector expressed in the local frame is defined as

$$\boldsymbol{\Omega} = 2\widehat{\mathbf{q}}^{*} \circ \dot{\widehat{\mathbf{q}}}, \tag{36}$$

which yields the expressions for the nodal angular velocities of elements I and II at the joint

$$\overline{\boldsymbol{\Omega}}^{\mathrm{I}} = 2\widehat{\mathbf{q}}^{\mathrm{I}*} \circ \dot{\widehat{\mathbf{q}}}^{\mathrm{I}} \qquad \text{and} \qquad \overline{\boldsymbol{\Omega}}^{\mathrm{II}} = 2\widehat{\mathbf{q}}^{\mathrm{II}*} \circ \dot{\widehat{\mathbf{q}}}^{\mathrm{II}}.$$

After considering (34), we have

$$\overline{\boldsymbol{\Omega}}^{\mathrm{I}} = 2\widehat{\mathbf{q}}_0^{\mathrm{I}*} \circ \widehat{\mathbf{k}}^{\mathrm{I}*} \circ \dot{\widehat{\mathbf{k}}}^{\mathrm{I}} \circ \widehat{\mathbf{q}}_0^{\mathrm{I}},$$

$$\overline{\boldsymbol{\Omega}}^{\mathrm{II}} = 2\widehat{\mathbf{q}}_0^{\mathrm{II}*} \circ \widehat{\mathbf{k}}^{\mathrm{II}*} \circ \dot{\widehat{\mathbf{k}}}^{\mathrm{II}} \circ \widehat{\mathbf{q}}_0^{\mathrm{II}}.$$

Since the relative rotation $\widehat{\mathbf{k}}$ is continuous over the boundaries of elements, eq. (35), we are able to express the constraint relation between the boundary angular velocities

$$\widehat{\mathbf{q}}_0^{\mathrm{I}} \circ \overline{\boldsymbol{\Omega}}^{\mathrm{I}} \circ \widehat{\mathbf{q}}_0^{\mathrm{I}*} = \widehat{\mathbf{q}}_0^{\mathrm{II}} \circ \overline{\boldsymbol{\Omega}}^{\mathrm{II}} \circ \widehat{\mathbf{q}}_0^{\mathrm{II}*}. \tag{37}$$

For the clarity of further derivation, it is convenient to express (37) in terms of rotation matrices:

$$\mathbf{R}_0^{\mathrm{I}} \overline{\boldsymbol{\Omega}}^{\mathrm{I}} = \mathbf{R}_0^{\mathrm{II}} \overline{\boldsymbol{\Omega}}^{\mathrm{II}}, \tag{38}$$

where $\mathbf{R}_0^{\mathrm{I}}$ and $\mathbf{R}_0^{\mathrm{II}}$ denote the standard rotation matrices equivalent to quaternion-based rotations expressed with $\widehat{\mathbf{q}}_0^{\mathrm{I}}$ and $\widehat{\mathbf{q}}_0^{\mathrm{II}}$.

### B. Algorithmically enforced boundary conditions

A solution of two moment equilibrium equations (22) expressed at the same node, here formally written as

$$\mathcal{M}^{\mathrm{I}}\left(\overline{\boldsymbol{\Omega}}^{\mathrm{I}}\right) = \mathbf{0} \qquad \text{and} \qquad \mathcal{M}^{\mathrm{II}}\left(\overline{\boldsymbol{\Omega}}^{\mathrm{II}}\right) = \mathbf{0}, \tag{39}$$

needs to be found. The solution must also satisfy the algebraic constraint

$$\mathbf{R}_0^{\mathrm{I}} \overline{\boldsymbol{\Omega}}^{\mathrm{I}} - \mathbf{R}_0^{\mathrm{II}} \overline{\boldsymbol{\Omega}}^{\mathrm{II}} = 0. \tag{40}$$

Following the method of Lagrange multipliers the constraint equation is multiplied by a multiplier $\lambda$ and linearized. The corresponding partial derivatives are then added to the initial variational problem to obtain the weak form of Lagrange function. For the present case it reads

$$\mathcal{M}^{\mathrm{I}}\left(\overline{\boldsymbol{\Omega}}^{\mathrm{I}}\right) + \mathbf{R}_0^{\mathrm{I}}\lambda = \mathbf{0}, \tag{41}$$

$$\mathcal{M}^{\mathrm{II}}\left(\overline{\boldsymbol{\Omega}}^{\mathrm{II}}\right) - \mathbf{R}_0^{\mathrm{II}}\lambda = \mathbf{0}, \tag{42}$$

$$\mathbf{R}_0^{\mathrm{I}} \overline{\boldsymbol{\Omega}}^{\mathrm{I}} - \mathbf{R}_0^{\mathrm{II}} \overline{\boldsymbol{\Omega}}^{\mathrm{II}} = \mathbf{0}. \tag{43}$$

The method thus increases the size of the system and the computational demands. It introduces three additional scalar unknowns and three additional equations for each rigid joint

between two elements. To avoid this, we introduce the following change of variables describing the nodal rotation-related unknowns:

$$\overline{\mathbf{\Omega}}^{\mathrm{I}}_R = \mathbf{R}^{\mathrm{I}}_0 \overline{\mathbf{\Omega}}^{\mathrm{I}} \qquad \text{and} \qquad \overline{\mathbf{\Omega}}^{\mathrm{II}}_R = \mathbf{R}^{\mathrm{II}}_0 \overline{\mathbf{\Omega}}^{\mathrm{II}}. \tag{44}$$

Based on the substitution of unknowns (44), the method of Lagrange multipliers gives

$$\mathcal{M}^{\mathrm{I}}\left(\mathbf{R}^{\mathrm{I}T}_0 \overline{\mathbf{\Omega}}^{\mathrm{I}}_R\right) + \lambda = \mathbf{0}, \tag{45}$$

$$\mathcal{M}^{\mathrm{II}}\left(\mathbf{R}^{\mathrm{II}T}_0 \overline{\mathbf{\Omega}}^{\mathrm{II}}_R\right) - \lambda = \mathbf{0}, \tag{46}$$

$$\overline{\mathbf{\Omega}}^{\mathrm{I}}_R - \overline{\mathbf{\Omega}}^{\mathrm{II}}_R = \mathbf{0}. \tag{47}$$

The system (45)–(47) can be easily reduced since the nodal unknowns are now identical: $\overline{\mathbf{\Omega}}_R = \overline{\mathbf{\Omega}}^{\mathrm{I}}_R = \overline{\mathbf{\Omega}}^{\mathrm{II}}_R$. These new variables can be interpreted as the relative angular velocities in a relative local frame. It is important to observe that the equations (45)–(46) represent the moment equilibrium equations, both written with respect to the same fixed basis. This fact allows us to sum the first two equations which directly leads to the reduced moment equilibrium equation at the joint:

$$\mathcal{M}^{\mathrm{I}}\left(\overline{\mathbf{\Omega}}_R\right) + \mathcal{M}^{\mathrm{II}}\left(\overline{\mathbf{\Omega}}_R\right) = 0.$$

Translational degrees of freedom are left unchanged. The vector of nodal unknowns now becomes

$$\mathbf{y}_R = \left[\begin{array}{cccc} \overline{\mathbf{v}}_1 & \overline{\mathbf{\Omega}}_{R,1} & \cdots & \overline{\mathbf{v}}_M \quad \overline{\mathbf{\Omega}}_{R,M} \end{array}\right]^T,$$

while its iterative correction vector reads

$$\delta\mathbf{y}_R = \left[\begin{array}{cccc} \delta\overline{\mathbf{v}}_1 & \delta\overline{\mathbf{\Omega}}_{R,1} & \cdots & \delta\overline{\mathbf{v}}_M \quad \delta\overline{\mathbf{\Omega}}_{R,M} \end{array}\right]^T.$$

Note that the corrections of newly introduced variables (44) can still be directly summed up to the current iterative values. This property follows from the distributivity of multiplication of time-constant matrix $\mathbf{R}_0$ with the sum of angular velocity and its update. The original quantities $\overline{\mathbf{\Omega}}^{\mathrm{I}}$ and $\overline{\mathbf{\Omega}}^{\mathrm{II}}$ remain to be the interpolated quantities at the elements level. Hence in each iteration step $i$ the variables $\overline{\mathbf{\Omega}}^{\mathrm{I}}$ and $\overline{\mathbf{\Omega}}^{\mathrm{II}}$ are extracted from $\overline{\mathbf{\Omega}}^{\mathrm{I}}_R = \overline{\mathbf{\Omega}}^{\mathrm{II}}_R$ and applied for further calculations.

In order to adapt a block of the corresponding tangent stiffness matrix at an arbitrary boundary node of a element, we express it with four submatrices appurtenant to translational and rotational degrees of freedom

$$\mathbf{K}^{\mathrm{I}}_{\mathrm{node}} = \left[\begin{array}{cc} \mathbf{K}^{\mathrm{I}}_{\mathbf{vv}} & \mathbf{K}^{\mathrm{I}}_{\mathbf{v\Omega}} \\ \mathbf{K}^{\mathrm{I}}_{\mathbf{\Omega v}} & \mathbf{K}^{\mathrm{I}}_{\mathbf{\Omega\Omega}} \end{array}\right],$$

$$\mathbf{K}^{\mathrm{II}}_{\mathrm{node}} = \left[\begin{array}{cc} \mathbf{K}^{\mathrm{II}}_{\mathbf{vv}} & \mathbf{K}^{\mathrm{II}}_{\mathbf{v\Omega}} \\ \mathbf{K}^{\mathrm{II}}_{\mathbf{\Omega v}} & \mathbf{K}^{\mathrm{II}}_{\mathbf{\Omega\Omega}} \end{array}\right],$$

where $\mathbf{K}_{\mathbf{vv}}$ and $\mathbf{K}_{\mathbf{v\Omega}}$ denote the partial derivatives of (21) with respect to velocities and angular velocities, respectively. Similarly, $\mathbf{K}_{\mathbf{\Omega v}}$ and $\mathbf{K}_{\mathbf{\Omega\Omega}}$ denote the partial derivatives of (22). While the matrices $\mathbf{K}_{\mathbf{vv}}$ and $\mathbf{K}_{\mathbf{\Omega v}}$ are left unchanged, the derivatives with respect to angular velocities need to be transformed in accord with the newly introduced variable leading to

$$\tilde{\mathbf{K}}^{\mathrm{I}}_{\mathrm{node}} = \left[\begin{array}{cc} \mathbf{K}^{\mathrm{I}}_{\mathbf{vv}} & \mathbf{K}^{\mathrm{I}}_{\mathbf{v\Omega}} \left(\mathbf{R}^{\mathrm{I}}_0\right)^T \\ \mathbf{K}^{\mathrm{I}}_{\mathbf{\Omega v}} & \mathbf{K}^{\mathrm{I}}_{\mathbf{\Omega\Omega}} \left(\mathbf{R}^{\mathrm{I}}_0\right)^T \end{array}\right]$$

$$\tilde{\mathbf{K}}^{\mathrm{II}}_{\mathrm{node}} = \left[\begin{array}{cc} \mathbf{K}^{\mathrm{II}}_{\mathbf{vv}} & \mathbf{K}^{\mathrm{II}}_{\mathbf{v\Omega}} \left(\mathbf{R}^{\mathrm{II}}_0\right)^T \\ \mathbf{K}^{\mathrm{II}}_{\mathbf{\Omega v}} & \mathbf{K}^{\mathrm{II}}_{\mathbf{\Omega\Omega}} \left(\mathbf{R}^{\mathrm{II}}_0\right)^T \end{array}\right].$$

The above transformation allows the direct summation of nodal tangent matrices within the Boolean identification technique to be admissible for the chosen formulation:

$$\tilde{\mathbf{K}}_{\mathrm{node}} = \tilde{\mathbf{K}}^{\mathrm{I}}_{\mathrm{node}} + \tilde{\mathbf{K}}^{\mathrm{II}}_{\mathrm{node}}.$$

With this procedure only six variables per node are needed and computational complexity is only slightly increased due to transformation of tangent stiffness matrices and the reconstruction of average angular velocities at the element's level from the relative ones at the structural level. This procedure is done by applying a simple time-independent rotation. The main advantage, i.e., the additivity of the iterative and the interpolated unknowns, is preserved. The size of the problem for each element thus remains equal to $6N$, which means that on the structural level we need to solve $6(N \cdot E - n)$ equations, where $E$ denotes the number of elements and $n$ the number of rigid joints. To enforce the boundary conditions, the proposed method requires $n$ additional matrix products of the initial transposed rotation matrix, $\mathbf{R}^T_0$, and the relative angular velocity, $\overline{\mathbf{\Omega}}_R$. As we will show by numerical example, these costs are negligible with respect to the overall numerical procedure.

## VI. Numerical studies

The applicability and excellent performance of the proposed method will be demonstrated by standard benchmark examples for flexible beam-like structures with finite strains where the structure undergoes large displacements and rotations. Equidistant discretization points were chosen for spatial discretization and standard Lagrangian polynomials were taken to be interpolation functions. Integrals were evaluated numerically using the Gaussian quadrature rule. The Newton-Raphson iteration scheme was terminated when the Euclidean norm of the vector of corrections of all primary unknowns was under $10^{-9}$. The geometric and material data chosen in the examples are

$$\begin{aligned} EA = GA_2 = GA_3 &= 10^6 \text{ N}, \\ GI_1 = EI_2 = EI_3 &= 10^3 \text{ Nm}^2, \\ \rho A &= 1 \text{ kg/m}. \end{aligned}$$

Other data are provided separately for each example.

### A. Free flight of a beam: the computational performance

In our first example, we analyse the computational performance of the present approach when solving a problem similar to the one introduced by Simo and Vu-Quoc [18]. The beam is initially inclined and subjected to a piecewise linear point force $f_X$ and point moments $h_Y$ and $h_Z$ at the lower end, as

shown in Figure 3. The mass-inertia matrix of the cross-section is taken to be: $\mathbf{J}_\rho = \mathrm{diag}\,[\ 10 \quad 10 \quad 10\ ]\ \mathrm{kg\,m}$.

For this particular problem, all elements have equal initial orientations. A simple Boolean identification of degrees of freedom is therefore reasonable even if angular velocities in local frame description are the primary unknowns, which is the case in our approach. This allows us to solve the problem in two different ways: i) with Boolean identification and ii) using the proposed algorithm. By doing so, we will be able to compare the computational times and demonstrate the demands of the presented algorithm. Note that the Boolean identification is not appropriate when solving problems, where elements have different initial inclinations, which limits its applicability and generality.

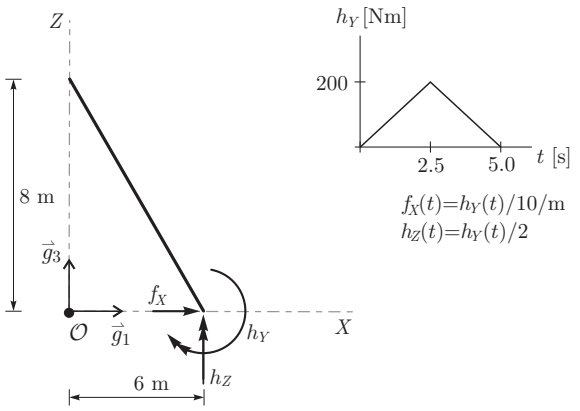


Figure 3. Unsupported beam that is initially straight but inclined.

To compare both methods, a dense mesh of 100 linear elements has been used. For this problem a small number of elements would be sufficient, but by increasing their number the complexity of the overall algorithm raises so the additional demands of the proposed algorithm can be easier observed. Besides that, the computational error of the results becomes negligible with very dense mesh. The average computational times of the same evaluation in seconds are presented in Table I.

TABLE I. COMPUTATIONAL TIMES OF INITIALLY STRAIGHT BEAM.

| *Method* | *initial time step* | *ten time steps* |
|---|---|---|
| Boolean identification | 3.415 | 42.820 |
| proposed algorithm | 3.508 | 34.011 |

We can observe that computational times of the proposed method are only slightly larger after the first time step. However, in the time stepping procedure the proposed algorithm behaves better since the newly introduced relative velocities seem to be more suitable computational unknowns, which leads to a lower number of total iterations needed and, therefore, lower computational times.

### *B. Large deflections of right-angle cantilever*

This classical example introduced by Simo and Vu-Quoc [18] was studied by many authors. A right-angle cantilever beam is subjected to a triangular pulse out-of-plane load at the elbow, see Figure 4. Each part of the cantilever is dicretized with two third-order elements. A dynamic response of the cantilever involves very large magnitudes of displacements and rotations together with finite strains. After removal of the external force, the cantilever undergoes free vibrations and the total mechanical energy of the cantilever should remain constant. Therefore, the stability of the algorithm is here checked through the energy behaviour. The centroidal mass-inertia matrix of the cross-section is diagonal: $\mathbf{J}_\rho = \mathrm{diag}\,[\ 20 \quad 10 \quad 10\ ]\ \mathrm{kg\,m}$. Originally, the solution was computed on the time interval $[0, 30]$ s with fixed time step $0.25$ s, later the interval was extended to $[0, 50]$ s by Jelenić and Crisfield [37] claiming that most of the algorithms encounter numerical stability problems between times 30 s and

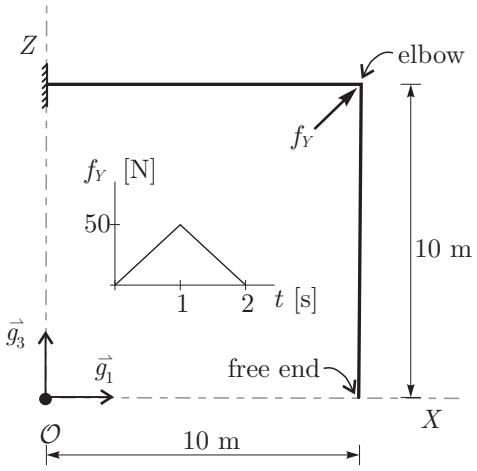


Figure 4. The right-angle cantilever subjected to out-of-plane loading.

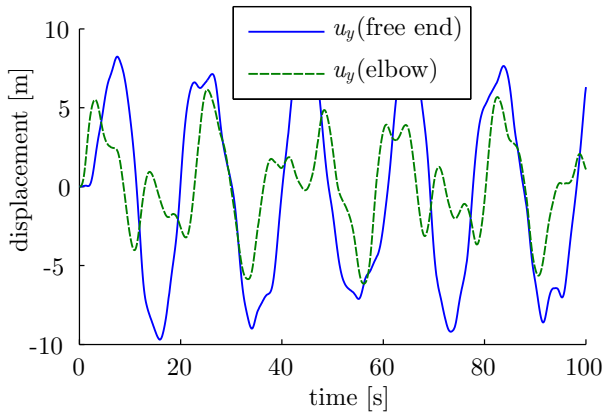


Figure 5. The out-of-plane displacements at free-end and at elbow for the right-angle cantilever.

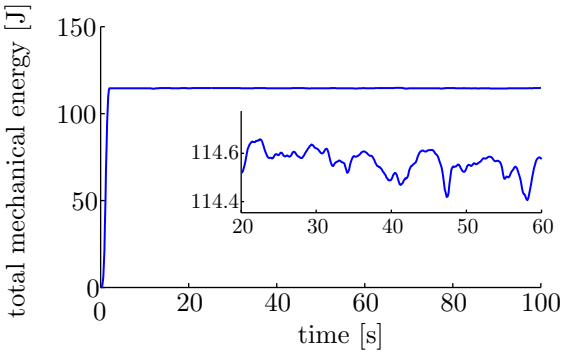


Figure 6. The time history of the total mechanical energy for the right-angle cantilever.

50 s. Here on a longer time interval $[0, 100]$ s solution was obtained without any numerical problems noticed, see Figure 5. However, the time step used had to be reduced by half, $h = 0.125$ s, otherwise the iteration could not achieve the prescribed tolerance condition at time 51.5 s. From Figure 6 we can observe almost constant total mechanical energy after time $t = 5$ s; only slight discrepancy of about 0.2% can be observed, which indicates good stability of calculations. The present results on the time interval $[0, 30]$ s agree well with the results reported by other authors.

### C. Large overall motion of a flexible cross-like structure

The large overall motion of completely free "cross" was first presented by Simo et al. [38] to illustrate the performance of the algorithm when calculating the dynamics response of a reticulated structure. The geometry and the applied external out-of plane forces are depicted in Figure 7. The centroidal mass-inertia matrix of the cross-section is taken to be $\mathbf{J}_\rho = \text{diag}\,[\ 10\quad 10\quad 10\ ]\ \text{kg m}$.

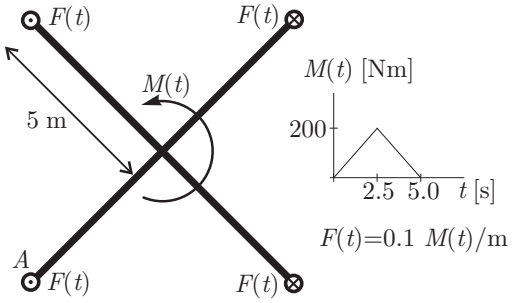


Figure 7. The geometry and the loading of the "cross".

In this example, four finite elements are rigidly connected at the central point sharing the same velocities and the same relative angular velocities. Thus, it is very suitable for the demonstration of the appropriateness of the proposed approach. The solution was computed on a very large time interval $[0, 1000]$ s with time step $h = 0.1$ s. We observed perfect quadratic convergence of the algorithm during the whole calculation. Because the interval of calculation is so extremely long we present only displacements on short intervals at the beginning and at the end of calculation, see Figure 8.

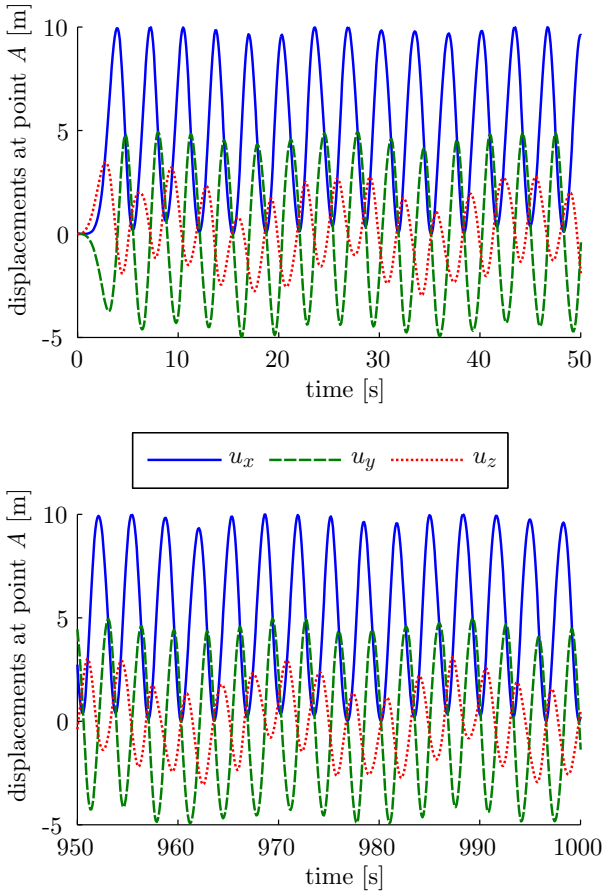


Figure 8. The displacements of the "cross" at point A at the beginning and at the end of calculation.

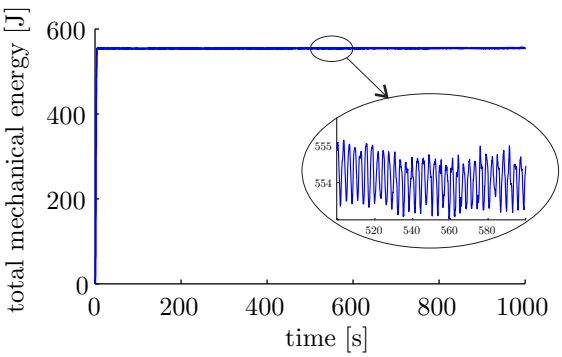


Figure 9. The time history of the total mechanical energy for the "cross".

After removal of external forces at time $t = 5$ s the cross vibrates freely in a periodic-like dynamic pattern and the total

mechanical energy is almost constant as expected, see Figure 9. The calculations remain stable even after 10 000 time steps. More detailed results are, to author's best knowledge, not available in literature. However, almost the same response is obtained by finer mesh and/or smaller time step indicating that the computational errors for this problem are small.

## VII. Conclusion

A novel finite-element approach for the beam dynamics has been presented. The proposed method exploits the benefits of the favourable properties of angular velocity in the local frame description. The computational advantages of the quaternion representation of rotations are preserved, but additionally with the replacement of the primary unknowns we gain the considerable increase of numerical stability and robustness of the model without any other measures needed. The issue of the continuity of the structural unknowns over the element boundaries has been resolved with minimal computational cost. The classical benchmark examples demonstrate the excellent performance of the proposed method. Even for large number of time steps a reliable results were obtained and almost perfect preservation of the total mechanical energy is gained for sufficiently dense meshes and sufficiently small time-step sizes.

## Acknowledgment

This work was supported by the Slovenian Research Agency through the research programme P2-0260. The support is gratefully acknowledged.

## References

[1] E. Zupan and D. Zupan, "On the Implementation of Novel Velocity-based 3D Beam: Compatibility of Angular Velocities Over the FEM Boundaries," ADVCOMP 2016, The Tenth International Conference on Advanced Engineering Computing and Applications in Sciences, pp. 17–22.

[2] S. S. Antman, Nonlinear Problems of Elasticity, 2nd ed. Berlin: Springer, 2005.

[3] E. Reissner, "On finite deformations of space-curved beams," Z. Angew. Math. Phys., vol. 32, no. 6, pp. 734–744, 1981.

[4] J. C. Simo, "A finite strain beam formulation - the three-dimensional dynamic problem. Part I." Comput. Meth. Appl. Mech. Eng., vol. 49, no. 1, pp. 55–70, 1985.

[5] J. M. Battini and C. Pacoste, "Co-rotational beam elements with warping effects in instability problems," Comput. Meth. Appl. Mech. Eng., vol. 191, no. 17-18, pp. 1755–1789, 2002.

[6] O. A. Bauchau and N. J. Theron, "Energy decaying scheme for non-linear beam models," Comput. Meth. Appl. Mech. Eng., vol. 134, no. 1-2, pp. 37–56, 1996.

[7] P. Betsch and P. Steinmann, "Frame-indifferent beam finite elements based upon the geometrically exact beam theory," Int. J. Numer. Methods Eng., vol. 54, no. 12, pp. 1775–1788, 2002.

[8] O. Brüls, A. Cardona, and M. Arnold, "Lie group generalized-alpha time integration of constrained flexible multibody systems," Mech. Mach. Theory, vol. 48, pp. 121–137, 2012.

[9] A. Cardona and M. Géradin, "A beam finite-element non-linear theory with finite rotations," Int. J. Numer. Methods Eng., vol. 26, no. 11, pp. 2403–2438, 1988.

[10] M. A. Crisfield, "A consistent corotational formulation for nonlinear, 3-dimensional, beam-elements," Comput. Meth. Appl. Mech. Eng., vol. 81, no. 2, pp. 131–150, 1990.

[11] L. A. Crivelli and C. A. Felippa, "A 3-dimensional nonlinear Timoshenko beam based on the core-congruential formulation," Int. J. Numer. Methods Eng., vol. 36, no. 21, pp. 3647–3673, 1993.

[12] A. Ibrahimbegovic, "On finite-element implementation of geometrically nonlinear Reissner beam theory - 3-dimensional curved beam elements," Comput. Methods Appl. Mech. Eng., vol. 122, no. 1-2, pp. 11–26, 1995.

[13] G. Jelenić and M. Saje, "A kinematically exact space finite strain beam model - finite-element formulation by generalized virtual work principle," Comput. Methods Appl. Mech. Eng., vol. 120, no. 1-2, pp. 131–161, 1995.

[14] H. Lang, J. Linn, and M. Arnold, "Multi-body dynamics simulation of geometrically exact Cosserat rods," Multibody Syst. Dyn., vol. 25, no. 3, pp. 285–312, 2011.

[15] E. Zupan, M. Saje, and D. Zupan, "The quaternion-based three-dimensional beam theory," Comput. Meth. Appl. Mech. Eng., vol. 198, no. 49-52, pp. 3944–3956, 2009.

[16] P. Crouch and R. Grossman, "Numerical-integration of ordinary differential-equations on manifolds," J. Nonlinear Sci., vol. 3, no. 1, 1993, pp. 1–33.

[17] C. Bottasso and M. Borri, "Integrating finite rotations," Comput. Meth. Appl. Mech. Eng., vol. 164, no. 3-4, 1998, pp. 307–331.

[18] J. C. Simo and L. Vu-Quoc, "On the dynamics in space of rods undergoing large motions - a geometrically exact approach," Comput. Meth. Appl. Mech. Eng., vol. 66, no. 2, 1988, pp. 125–161.

[19] H. Munthe-Kaas, "Runge-Kutta methods on Lie groups," Bit, vol. 38, no. 1, 1998, pp. 92–111.

[20] H. Munthe-Kaas, , "High order Runge-Kutta methods on manifolds," Appl. Numer. Math., vol. 29, no. 1, pp. 115–127, 1999.

[21] A. Zanna, "Collocation and relaxed collocation for the FER and the Magnus expansions," SIAM J. Numer. Anal., vol. 36, no. 4, 1999, pp. 1145–1182.

[22] J. Argyris and V. Poterasu, "Large rotations revisited application of Lie-algebra," Comput. Meth. Appl. Mech. Eng., vol. 103, no. 1-2, pp. 11–42, 1993.

[23] C. Bottasso, "A non-linear beam space-time finite element formulation using quaternion algebra: interpolation of the Lagrange multipliers and the appearance of spurious modes," Comput. Mech., vol. 10, no. 5, pp. 359–368, 1992.

[24] S. Kehrbaum and J. H. Maddocks, "Elastic rods, rigid bodies, quaternions and the last quadrature," Philos. Trans. R. Soc. A-Math. Phys. Eng. Sci., vol. 355, no. 1732, pp. 2117–2136, 1997.

[25] F. McRobie and J. Lasenby, "Simo-Vu Quoc rods using Clifford algebra," Int. J. Numer. Methods Eng., vol. 45, no. 4, pp. 377–398, 1999.

[26] S. Ghosh and D. Roy, "Consistent quaternion interpolation for objective finite element approximation of geometrically exact beam," Comput. Meth. Appl. Mech. Eng., vol. 198, no. 3-4, pp. 555–571, 2008.

[27] H. Lang and M. Arnold, "Numerical aspects in the dynamic simulation of geometrically exact rods," Appl. Numer. Math., vol. 62, no. 10, SI, pp. 1411–1427, 2012.

[28] E. Zupan, M. Saje, and D. Zupan, "Quaternion-based dynamics of geometrically nonlinear spatial beams using the Runge-Kutta method," Finite Elem. Anal. Des., vol. 54, pp. 48–60, 2012.

[29] E. Zupan, M. Saje, and D. Zupan, "Dynamics of spatial beams in quaternion description based on the Newmark integration scheme," Comput. Mech., vol. 51, no. 1, pp. 47–64, 2013.

[30] M. E. Hosea and L. F. Shampine, "Analysis and implementation of TR-BDF2," Appl. Numer. Math., vol. 20, no. 1-2, pp. 21–37, 1996.

[31] J. P. Ward, Quaternions and Cayley Numbers. Dordrecht–Boston–London: Kluwer Academic Publishers, 1997.

[32] H. Lang and J. Linn, "Lagrangian field theory in space-time for geometrically exact Cosserat rods," ITWM, Kaiserslautern, Reports of the ITWM, no. 150, 2003.

[33] S. S. Antman, "Invariant dissipative mechanisms for the spatial motion of rods suggested by artificial viscosity," J. Elast., vol. 70, no. 1-3, pp. 55–64, 2003.

[34] D. Hodges, "Geometrically exact, intrinsic theory for dynamics of curved and twisted anisotropic beams," AIAA J., vol. 41, no. 6, pp. 1131–1137, 2003.

[35] P. Cesarek and D. Zupan, "On the stability of Lie group time integration in multibody dynamics," in The 2nd Joint Conference on Multibody System Dynamics, May 29–June 1, 2012, Stuttgart, Germany. Book of Abstracts, H. M. Götz and P. Ziegler, Eds., pp. 42–43, 2012.

[36] E. Zupan and D. Zupan, "Velocity-based approach in non-linear dynamics of three-dimensional beams with enforced kinematic compatibility," Comput. Meth. Appl. Mech. Eng., vol. 310, pp. 406–428, 2016.

[37] G. Jelenić and M. A. Crisfield, "Geometrically exact 3D beam theory: implementation of a strain-invariant finite element for statics and dynamics," Comput. Meth. Appl. Mech. Eng., vol. 171, no. 1-2, pp. 141–171, 1999.

[38] J. C. Simo, N. Tarnow, and M. Doblare, "Nonlinear dynamics of 3-dimensional rods - exact energy and momentum conserving algorithms," Int. J. Numer. Methods Eng., vol. 38, no. 9, pp. 1431–1473, 1995.